Editors' Suggestion | Featured in Physics

Kerr-Enhanced Optical Spring

Sotatsu Otabe,[1,2,*] Wataru Usukura,[1] Kaido Suzuki,[1] Kentaro Komori,[3,4] Yuta Michimura,[5,3] Ken-ichi Harada,[1] and Kentaro Somiya[1]

[1]*Department of Physics, Tokyo Institute of Technology, Meguro, Tokyo 152-8550, Japan*
[2]*Institute of Innovative Research, Tokyo Institute of Technology, Yokohama, Kanagawa 226-8503, Japan*
[3]*Research Center for the Early Universe (RESCEU), Graduate School of Science, University of Tokyo, Bunkyo, Tokyo 113-0033, Japan*
[4]*Department of Physics, University of Tokyo, Bunkyo, Tokyo 113-0033, Japan*
[5]*LIGO Laboratory, California Institute of Technology, Pasadena, California 91125, USA*

(Received 31 October 2023; accepted 20 February 2024; published 4 April 2024)

We propose and experimentally demonstrate the generation of enhanced optical springs using the optical Kerr effect. A nonlinear optical crystal is inserted into a Fabry-Perot cavity with a movable mirror, and a chain of second-order nonlinear optical effects in the phase-mismatched condition induces the Kerr effect. The optical spring constant is enhanced by a factor of 1.6 ± 0.1 over linear theory. To our knowledge, this is the first realization of optomechanical coupling enhancement using a nonlinear optical effect, which has been theoretically investigated to overcome the performance limitations of linear optomechanical systems. The tunable nonlinearity of demonstrated system has a wide range of potential applications, from observing gravitational waves emitted by binary neutron star postmerger remnants to cooling macroscopic oscillators to their quantum ground state.

DOI: 10.1103/PhysRevLett.132.143602

Introduction.—In 2017, gravitational waves from a binary neutron star merger were observed for the first time [1], and electromagnetic telescopes identified its counterpart [2]. The multimessenger observations thus realized have provided several remarkable astronomical insights, including the origin of short gamma-ray bursts [3], synthesis of very heavy elements via the r process [4], and novel independent measurements of the Hubble constant [5]. However, the high-frequency gravitational waves in the 2–4 kHz band, which are predicted to be emitted by remnants possibly formed after a binary merger [6,7], have not been observed because they lie outside the bandwidth of modern gravitational wave detectors (GWDs). Gravitational waves emitted from binary neutron star postmerger remnants contain critical information regarding high-density nuclear materials, which cannot be accessed via terrestrial experiments and is essential for determining the equation of state for neutron stars [8]. The internal structure exploration of neutron stars is a primary motivation for constructing third-generation GWDs [9,10] because postmerger signals are only observed once every few decades by second-generation GWDs [11–13]. Interferometric geometry modification of second- or third-generation GWDs for specialization in the 2–4 kHz band has also been proposed [14–17].

Signal amplification using an optical spring is a promising technique for improving specific band sensitivity in GWDs [18–21]. An optical spring can be generated by detuning the optical cavity to create a proportional relationship between the radiation pressure force and the test mass displacement. Under the constraint of a fixed detector bandwidth, the optical spring resonant frequency is determined by the intracavity light power [22–24] and is limited to approximately 100 Hz for second-generation GWDs [21]. Generally, improving the impact of the optical spring is challenging because increasing intracavity power results in harmful phenomena, including thermal lensing [11,25] or parametric instability [26,27]. To address this problem, implementation of a technique called intracavity squeezing, which can expand the bandwidth of the detector [28–32], has been investigated to increase the optical spring resonant frequency to several kHz [33–35]. This technique actively increases the signal amplification ratio of the cavity using intracavity nonlinear optical effects (NOEs) and enhances the optical spring constant without changing the intracavity power. The intracavity signal amplification method, which directly enhances optomechanical coupling, fundamentally differs from the input squeezing technique [36–40] currently used for practical GWDs [41,42], and these techniques can be used in combination [43].

It is worth noting that enhanced optomechanical coupling has been extensively researched beyond the context of GWDs. Intracavity squeezing has the potential to cool an optomechanical oscillator to the ground state in the unresolved sideband regime [44–46], which closely relates to enhancing optical damping (i.e., the imaginary component of the complex optical spring constant) using NOEs. Moreover, the application of enhanced optomechanical

coupling via intracavity NOEs to generate strong mechanical squeezing [47–49], manipulate normal-mode splitting [50,51], and realize single-photon quantum processes [52,53] has been theoretically investigated. Direct observation of enhanced optomechanical coupling represents a significant step toward achieving the full potential of future optomechanical systems.

This Letter reports on observations from an experimental demonstration focused on optical spring enhancement via NOEs, which is essential for intracavity signal amplification systems. We induced the NOE in a Fabry-Perot type optomechanical cavity. Among the various candidates for NOEs capable of generating squeezed states [54], our research revealed that the optical Kerr effect is a promising approach. This effect provides significant signal amplification effects while maintaining sufficient intracavity power, and thus, strong optomechanical coupling can be generated.

Kerr-enhanced optomechanical system.—We investigate a system wherein the Kerr medium is inserted into the optomechanical cavity [Fig. 1(a)]. The dynamics of this system can be described as the sum of the optomechanical Hamiltonian [55,56] and Kerr Hamiltonian $\hat{H}_{\mathrm{Kerr}} = (\hbar/2)\chi(\hat{a}^\dagger)^2\hat{a}^2$ [57]. Here, $\hbar$ is the reduced Planck constant, χ is the quantity proportional to the nonlinear susceptibility of the Kerr medium, and $\hat{a}^\dagger$ and $\hat{a}$ are the creation and annihilation operators of the optical mode, respectively. The differential equation for the complex light-field amplitude $a(t)$ in the cavity without intracavity losses can be written as

$$\dot{a} = [i\Delta' + iGx - i\chi n - \gamma]a + \sqrt{2\gamma}a_{\mathrm{in}}, \tag{1}$$

where x is the sum of the mechanical and photothermal displacements [58,59], G is the optomechanical frequency shift per displacement, and a_{in} is the amplitude of the drive laser. The Kerr effect practically changes the angular frequency of cavity detuning Δ' proportionally to the intracavity photon number $n(t) = |a(t)|^2$, but it does not affect the cavity decay rate γ.

Let us make a linear approximation as $a(t) = \bar{a} + \delta a(t)$ and $x(t) = \bar{x} + \delta x(t)$ to examine the behavior of the light-field amplitude around a stable point. The intracavity power P can be defined by the average number of photons inside the cavity $\bar{n} = |\bar{a}|^2$, calculated from the zero-order terms as

$$P = \frac{\hbar\omega_0 c}{2L}\bar{n} = \frac{2\mathcal{F}}{\pi}\frac{1}{1+\xi^2}P_0, \tag{2}$$

where ω_0 is the angular frequency of the carrier light, c is the speed of light, L is the half cycle length of the cavity, $\mathcal{F}$ is the cavity finesse, and P_0 is the incident power of the carrier light on the cavity. The normalized cavity detuning of the Kerr system $\xi = \xi_0 + \xi_{\mathrm{K}}$ consists of two components, where $\gamma\xi_0 = \Delta' + G\bar{x}$ is the shifted cavity detuning of the linear optomechanical system, and $\gamma\xi_{\mathrm{K}} = -\chi\bar{n}$ is the cavity detuning derived from the refractive index change due to the Kerr effect. The asymmetry of the cavity spectrum of the Kerr system [Fig. 1(b)] is a consequence of the nonlinear phase shift, which is proportional to the intracavity power.

The motion of a movable mirror in the optomechanical cavity is dominated by the radiation pressure force modified by the Kerr effect. We focus on the optical spring, a phenomenon resulting from the proportionality of the radiation pressure force to the displacement of the test mass. The optical spring constant in a linear system is proportional to the product of the intracavity power and cavity finesse, which generally has technical limits. In contrast, in the Kerr system, a drastic gradient of the radiation pressure force exists compared to a linear system. Therefore, we can generate an optical spring enhanced by the Kerr effect without changing the intracavity power or the cavity linewidth [Fig. 1(c)]. The complex optical spring constant for the angular frequency Ω is obtained from simultaneous equations for the first-order micro terms of the light-field amplitude and cavity length, which can be written as [60]

$$K_{\mathrm{opt}}(\Omega) = \frac{4\omega_0 P}{Lc\gamma}\frac{\xi}{(1+i\Omega/\gamma)^2 + \xi^2 + 2\xi\xi_{\mathrm{K}}}. \tag{3}$$

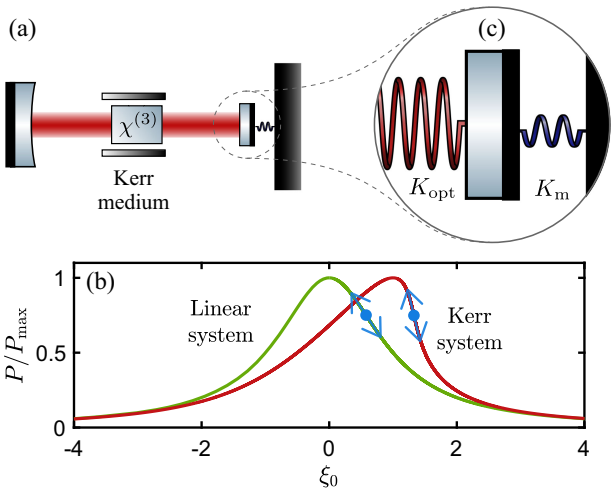

FIG. 1. (a) Schematic of an optomechanical system whose coupling is enhanced by the optical Kerr effect. An optical crystal with third-order nonlinearity $\chi^{(3)}$ (Kerr medium) is inserted into a laser-driven optical cavity with a movable-end mirror. (b) Theoretical intracavity power curve. Linear and Kerr systems correspond to the cases of Kerr gains at $\zeta = 0$ and $\zeta = -1$, respectively. The vertical axis is normalized by the intracavity power at resonance $P_{\mathrm{max}} = 2\mathcal{F}P_0/\pi$. (c) Schematic of the mechanical and enhanced optical springs, whose complex spring constants are K_{m} and K_{opt}, respectively. The positive optical spring resulting from the radiation pressure restoring force is enhanced by signal amplification due to the Kerr effect with $\zeta < 0$.

The real and imaginary components of Eq. (3) correspond to the optical spring and damping constant, respectively. The dimensionless Kerr gain ζ, which does not depend on cavity detuning, follows from Eq. (2) as

$$\zeta = (1+\xi^2)\xi_K = -\frac{2\chi P_0}{\gamma^2 \hbar \omega_0}. \tag{4}$$

When ζ exceeds a threshold value of $\zeta_0 = -8/(3\sqrt{3}) \sim -1.54$, multiple intracavity powers correspond to a single cavity detuning, indicating that the cavity response enters a multistable state [28,61–63]. The signal amplification ratio due to the Kerr effect increases by approaching a multistable regime.

Experimental setup.—We used a bow-tie cavity containing a 10-mm-long nonlinear optical crystal at a beam waist with a radius of 40 μm [Fig. 2(a)]. The measured finesse of this cavity is $\mathcal{F} \simeq 100 \pm 10$, which agrees with the design value. One of the mirrors constituting the cavity was small with a weight of 280 mg and diameter of 6.35 mm, suspended by a double spiral spring [Fig. 2(b)] with a resonant frequency of 14.0 ± 0.1 Hz and mechanical Q factor of 193 ± 3. This mirror was also coupled to an optical spring, allowing the precise measurement of the resonant frequencies of the composite spring.

NOEs were induced in phase-mismatched conditions. Figures 2(c) and 2(d) shows the dependence of the maximum transmitted power of the carrier light on the crystal temperature. At the phase-matching temperature (34.2 °C), the majority of the carrier light was converted into the second harmonic wave, decreasing the transmitted power. When the crystal temperature exceeded this temperature, almost no second harmonic was generated at some temperatures (e.g., 39.6 °C), and this condition was denoted as a phase mismatch. The second harmonic generation (SHG) processes are induced even in the phase-mismatched condition. However, the phases of the second harmonics were misaligned at each location in the crystal because the second harmonics propagate at a different speed than the fundamental wave. The generated second harmonics were canceled and reconverted into the fundamental wave with a different phase from the original. A chain of second-order NOEs induces a phase shift of the fundamental wave proportional to incident intensity, which is equivalent to the optical Kerr effect [68,69]. The effective velocity difference between the fundamental and second harmonics, and thus the effective nonlinear susceptibility χ, depends on the crystal temperature. At temperatures slightly different from other phase-mismatched conditions (e.g., 45.4 °C), the intracavity loss due to the SHG effect was equivalent to that of the first phase-mismatched condition. We compared the difference in optical spring constants for different Kerr gains by measuring them at temperatures with similar intracavity losses.

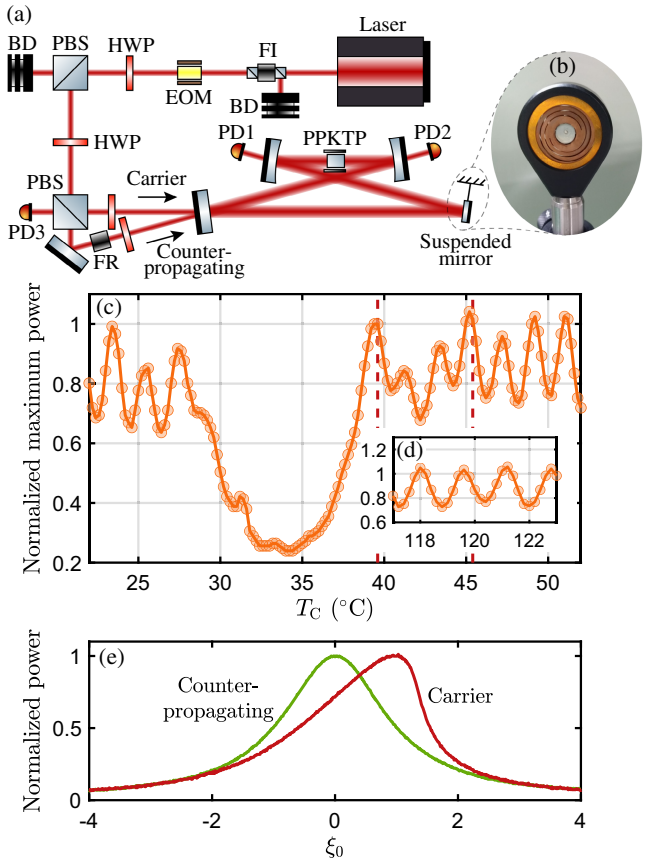

FIG. 2. (a) Experimental setup. Light emitted from a 1064 nm Nd:YAG laser passed through a Faraday isolator (FI) and an electro-optic modulator (EOM) and was attenuated by a half-wave plate (HWP), polarizing beam splitter (PBS), and beam damper (BD). A periodically poled $KTiOPO_4$ (PPKTP) crystal was inserted into the cavity to induce NOEs. (b) Image of a small mirror suspended by a double spiral spring. A magnet was attached to the back of the mirror, and the cavity length was varied through a coil magnet actuator. (c),(d) Transmitted light power at resonance versus crystal temperature T_C. The vertical axes are normalized by the transmitted light power at resonance in the first phase-mismatched condition (39.6 °C). The red dotted lines indicate the setting temperature for the optical spring constant measurement. The temperatures producing the phase-mismatched conditions remain periodically present in the high-temperature region, as shown in (d). (e) Measured cavity spectra. The horizontal axis was normalized by the half width at half maximum of the counterpropagating light power.

We injected light bidirectionally into the cavity. The transmitted carrier and counterpropagating light were measured using photodetectors (PDs) 1 and 2, and a Faraday rotator (FR) was used to measure the reflected carrier light with PD3. Figure 2(e) shows the transmitted light power of the carrier and the counterpropagating light under the first phase-mismatched condition, with input powers of 530 and 50 mW, respectively. Although no essential difference exists between these two paths, we can

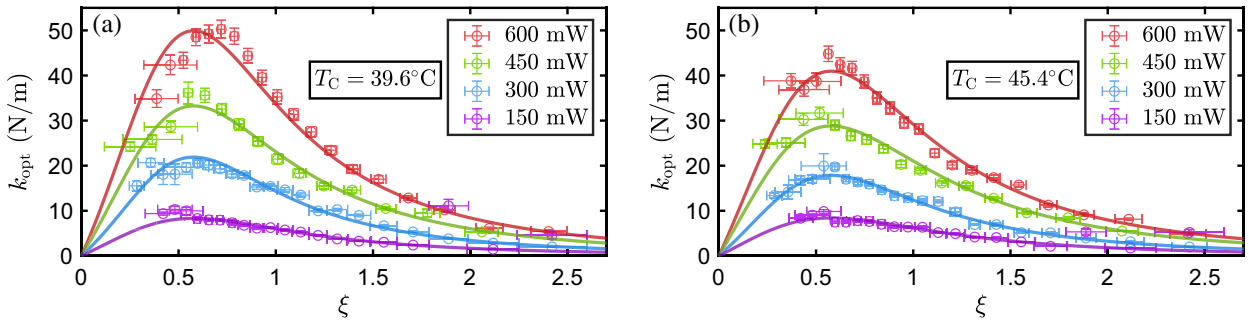

FIG. 3. (a),(b) Estimation of the optical spring constant $k_{opt} = K_{opt}(0)$. The input power P_0 was set to 600, 450, 300, and 150 mW, and the cavity detuning ξ was finely varied. The crystal temperature T_C was 39.6 °C for (a) and 45.4 °C for (b). The circles with error bars represent the estimated optical spring constants obtained from the transfer function measurements, and the solid lines in each color show the fitting results with the Kerr gain ζ and the maximum value of the optical spring constant for the linear theory $k_{opt-0} = K_{opt}(0)|_{\zeta=0,\xi=1/\sqrt{3}}$ as parameters.

examine the impact of the Kerr effect by injecting light of approximately 1 order of magnitude different powers into each path. The counterpropagating light is hardly affected by the Kerr effect and shows a Lorentzian curve, while the carrier light spectrum indicates that a nonlinear refractive index has been induced. This measurement was performed by inserting the crystal at an inclination relative to the cavity axis to avoid coupling of the carrier and counterpropagating light due to stray light on the antireflection coating. In this case, the first phase-mismatch temperature and Kerr gain changed. The crystal was reinstalled parallel to the cavity axis in subsequent measurements to obtain the highest possible Kerr gain.

Results.—We estimated the optical spring constant by applying a force to the test mass and then measuring the change in the cavity length from the reflected and transmitted light of the carrier path. The cavity length does not directly correspond to the displacement of the test mass owing to the photothermal effect in the nonlinear optical crystal. In our experimental system, it is critical to accurately measure the photothermal displacement, which rotates the quadrature of the optical spring [59,64,65]. Photothermal parameters can be estimated independently and highly accurately in an experimental setup not affected by an optical spring [58]. To compensate for the photothermal effect, we measured the photothermal displacement using a setup where a mirror with a piezoelectric element replaced the suspended mirror for each parameter used in the optical spring estimation process [60].

Figures 3(a) and 3(b) show the estimated results of the optical spring constant. The measured optical spring constants, for the same cavity detuning and input power, were larger when $T_C = 39.6$ °C, and a difference was observed at a higher input light power, reflecting that the Kerr gain was larger at 39.6 °C and proportional to the input light power. Slight systematic errors were expected due to changes in phase mismatching caused by thermal absorption in the nonlinear optical crystal [60]. Although the additional SHG loss was larger at 39.6 °C, the measured optical spring constant was also larger. Conclusively, the increase in optical spring constant owing to the Kerr effect was more significant than the decrease due to the SHG loss.

The signal amplification induced by the Kerr effect depends on the cavity detuning, and the difference from the linear system is maximized for $\xi = 1/\sqrt{3}$. This condition also provides the maximum value of the optical spring constant for both the Kerr and linear systems. Figure 4 shows the signal amplification ratio, i.e., the enhancement factor of the maximum optical spring constant compared to the linear theory. The estimated values for each input light power show clear differences between the two temperatures, indicating that the effective nonlinear susceptibility χ is adjustable. Conclusively, the optical spring is enhanced by the optical Kerr effect with a signal amplification ratio of up to 1.6 ± 0.1.

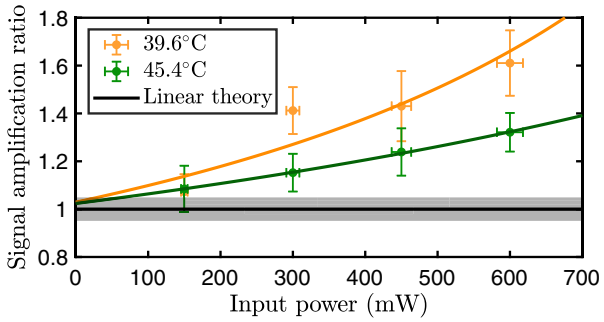

FIG. 4. Net signal amplification ratio obtained by normalizing the estimated maximum value of the optical spring constant using the relative input light power. The filled circles with error bars represent the estimated signal amplification ratio, and the solid lines in each color show the fitting with the Kerr theory. The vertical axis is normalized by k_{opt-0} estimated for $T_C = 39.6$ °C and $P_0 = 600$ mW, and the gray-filled area corresponds to its estimated error.

Discussion.—The experiment was based on the intracavity signal amplification method via an optical Kerr effect, which produced nontrivial amplification effects that could not be obtained by simply increasing the intracavity power or cavity finesse. The Kerr effect, estimated from optical spring measurements, was up to $-1.9\pm 0.2\times10^{-17}$ m^2/W in terms of the nonlinear refractive index. Our result was larger than the value of -2×10^{-18} m^2/W obtained in the previous study [62] because the periodic poling allowed the use of a larger nonlinear susceptibility [70]. In contrast, the nonlinear refractive index derived from the third-order nonlinearity of KTP was approximately 3×10^{-19} m^2/W [71], sufficiently smaller than the estimation error. The third-order nonlinearity could be observed with more precise measurements as a nonlinear refractive index independent of phase mismatching.

Further increase in the input light power could lead to multistability and considerably larger optical spring constants. From the fitting, the critical incident powers at which the optical spring constant diverges were predicted as 1.56 ± 0.37 W for $T_C = 39.6\,℃$ and 2.65 ± 0.05 W for $T_C = 45.4\,℃$. These conditions were sufficiently feasible, and we observed hysteresis in the spectrum, suggesting multistability, by replacing the input coupler and increasing the finesse to approximately 300 [60]. A higher signal amplification ratio would be observed by resolving the control instability.

In third-order NOEs, the Kerr gain is determined by the intracavity intensity and nonlinear susceptibility of the crystal. By inducing a chain of second-order NOEs, as in our experimental system, a variable Kerr gain can be achieved by varying the phase mismatch. Furthermore, the same scheme can be used to enhance backaction cooling in regions of $\xi < 0$ because the sign of the Kerr effect can be switched by decreasing the crystal temperature below the phase-matching condition [68,69].

Although experimental attempts have previously been made to enhance optomechanical coupling with optical parametric amplification [72,73], significant differences with the linear system were not observed because the SHG becomes dominant owing to the high intracavity power required to generate the optical spring. This property contrasts the Kerr scheme, wherein the effective signal amplification ratio can be increased with a higher carrier intensity. Moreover, the Kerr scheme is relatively easy to implement because this scheme does not add degrees of freedom that must be controlled. For GWDs, Kerr media shall be inserted into arm cavities with large beam size and high intracavity power [28]. The correspondence between the optical parametric amplification and Kerr schemes is detailed in the Supplemental Material [60] (see also references [66,67] therein).

Conclusion.—We constructed an intracavity signal amplification system based on the optical Kerr effect and succeeded in enhancing the optical spring constant by a factor of 1.6 ± 0.1. Our results correspond to an increase in the resonant frequency of the optical spring from 53 ± 1 Hz to 67 ± 3 Hz. A more significant signal amplification ratio could be achieved by approaching the multistable state and solving technical problems. The proposed scheme is easy to implement and provides a novel tunable parameter for optomechanical systems. We anticipate it will play a key role in the quantum manipulation of macroscopic optomechanical systems such as GWDs.

This work was supported by JST CREST (JPMJCR1873), Grant-in-Aid for JSPS Fellows (20J22778), and the Precise Measurement Technology Promotion Foundation. We would like to thank Jerome Degallaix and colleagues at LMA for providing us with a specially coated mirror and John Winterflood at UWA for designing the double spiral spring.

*Corresponding author: otabe@gw.phys.titech.ac.jp

[1] B. P. Abbott *et al.* (LIGO Scientific and Virgo Collaborations), Phys. Rev. Lett. **119**, 161101 (2017).
[2] B. P. Abbott *et al.*, Astrophys. J. Lett. **848**, L12 (2017).
[3] B. P. Abbott *et al.* (LIGO Scientific, Virgo, Fermi-GBM, and INTEGRAL Collaborations), Astrophys. J. Lett. **848**, L13 (2017).
[4] E. Pian *et al.*, Nature (London) **551**, 67 (2017).
[5] B. P. Abbott *et al.*, Nature (London) **551**, 85 (2017).
[6] L. Baiotti and L. Rezzolla, Rep. Prog. Phys. **80**, 096901 (2017).
[7] N. Sarin and P. D. Lasky, Gen. Relativ. Gravit. **53**, 59 (2021).
[8] M. Oertel, M. Hempel, T. Klähn, and S. Typel, Rev. Mod. Phys. **89**, 015007 (2017).
[9] M. Punturo *et al.*, Classical Quantum Gravity **27**, 194002 (2010).
[10] B. P. Abbott *et al.* (LIGO Scientific Collaboration), Classical Quantum Gravity **34**, 044001 (2017).
[11] G. M. Harry *et al.* (LIGO Scientific Collaboration), Classical Quantum Gravity **27**, 084006 (2010).
[12] F. Acernese *et al.* (VIRGO Collaboration), Classical Quantum Gravity **32**, 024001 (2014).
[13] K. Somiya (KAGRA Collaboration), Classical Quantum Gravity **29**, 124007 (2012).
[14] D. Martynov, H. Miao, H. Yang, F. H. Vivanco, E. Thrane, R. Smith *et al.*, Phys. Rev. D **99**, 102004 (2019).
[15] K. Ackley *et al.*, Pub. Astron. Soc. Aust. **37**, e047 (2020).
[16] J. Eichholz, N. A. Holland, V. B. Adya, J. V. van Heijningen, R. L. Ward, B. J. J. Slagmolen, D. E. McClelland, and D. J. Ottaway, Phys. Rev. D **102**, 122003 (2020).
[17] T. Zhang, H. Yang, D. Martynov, P. Schmidt, and H. Miao, Phys. Rev. X **13**, 021019 (2023).
[18] V. Braginsky and F. Khalili, Phys. Lett. A **257**, 241 (1999).
[19] A. Buonanno and Y. Chen, Classical Quantum Gravity **18**, L95 (2001).
[20] A. Buonanno and Y. Chen, Phys. Rev. D **64**, 042006 (2001).
[21] A. Buonanno and Y. Chen, Phys. Rev. D **65**, 042001 (2002).

[22] B. S. Sheard, M. B. Gray, C. M. Mow-Lowry, D. E. McClelland, and S. E. Whitcomb, Phys. Rev. A **69**, 051801(R) (2004).
[23] T. Corbitt, D. Ottaway, E. Innerhofer, J. Pelc, and N. Mavalvala, Phys. Rev. A **74**, 021802(R) (2006).
[24] T. Corbitt, Y. Chen, E. Innerhofer, H. Müller-Ebhardt, D. Ottaway, H. Rehbein, D. Sigg, S. Whitcomb, C. Wipf, and N. Mavalvala, Phys. Rev. Lett. **98**, 150802 (2007).
[25] B. Willke *et al.*, Classical Quantum Gravity **23**, S207 (2006).
[26] T. J. Kippenberg, H. Rokhsari, T. Carmon, A. Scherer, and K. J. Vahala, Phys. Rev. Lett. **95**, 033901 (2005).
[27] M. Evans, S. Gras, P. Fritschel, J. Miller, L. Barsotti, D. Martynov *et al.*, Phys. Rev. Lett. **114**, 161102 (2015).
[28] H. Rehbein, J. Harms, R. Schnabel, and K. Danzmann, Phys. Rev. Lett. **95**, 193001 (2005).
[29] M. Korobko, L. Kleybolte, S. Ast, H. Miao, Y. Chen, and R. Schnabel, Phys. Rev. Lett. **118**, 143601 (2017).
[30] H. Miao, N. D. Smith, and M. Evans, Phys. Rev. X **9**, 011053 (2019).
[31] M. Korobko, Y. Ma, Y. Chen, and R. Schnabel, Light Sci. Appl. **8**, 118 (2019).
[32] V. B. Adya, M. J. Yap, D. Töyrä, T. G. McRae, P. A. Altin, L. K. Sarre, M. Meijerink, N. Kijbunchoo, B. J. J. Slagmolen, R. L. Ward, and D. E. McClelland, Classical Quantum Gravity **37**, 07LT02 (2020).
[33] K. Somiya, Y. Kataoka, J. Kato, N. Saito, and K. Yano, Phys. Lett. A **380**, 521 (2016).
[34] M. Korobko, F. Khalili, and R. Schnabel, Phys. Lett. A **382**, 2238 (2018), special Issue in memory of Professor V. B. Braginsky.
[35] K. Somiya, K. Suzuki, S. Otabe, and K. Harada, Phys. Rev. D **107**, 122005 (2023).
[36] C. M. Caves, Phys. Rev. D **23**, 1693 (1981).
[37] H. J. Kimble, Y. Levin, A. B. Matsko, K. S. Thorne, and S. P. Vyatchanin, Phys. Rev. D **65**, 022002 (2001).
[38] Y. Zhao, N. Aritomi, E. Capocasa, M. Leonardi, M. Eisenmann, Y. Guo *et al.*, Phys. Rev. Lett. **124**, 171101 (2020).
[39] L. McCuller, C. Whittle, D. Ganapathy, K. Komori, M. Tse, A. Fernandez-Galiana *et al.*, Phys. Rev. Lett. **124**, 171102 (2020).
[40] F. Acernese *et al.* (Virgo Collaboration), Phys. Rev. Lett. **131**, 041403 (2023).
[41] M. Tse, H. Yu, N. Kijbunchoo, A. Fernandez-Galiana, P. Dupej, L. Barsotti *et al.*, Phys. Rev. Lett. **123**, 231107 (2019).
[42] F. Acernese *et al.* (Virgo Collaboration), Phys. Rev. Lett. **123**, 231108 (2019).
[43] M. Korobko, J. Südbeck, S. Steinlechner, and R. Schnabel, Phys. Rev. Lett. **131**, 143603 (2023).
[44] S. Huang and G. S. Agarwal, Phys. Rev. A **79**, 013821 (2009).
[45] M. Asjad, N. E. Abari, S. Zippilli, and D. Vitali, Opt. Express **27**, 32427 (2019).
[46] J.-H. Gan, Y.-C. Liu, C. Lu, X. Wang, M. K. Tey, and L. You, Laser Photonics Rev. **13**, 1900120 (2019).
[47] G. S. Agarwal and S. Huang, Phys. Rev. A **93**, 043844 (2016).
[48] B. Xiong, X. Li, S.-L. Chao, Z. Yang, R. Peng, and L. Zhou, Ann. Phys. (Berlin) **532**, 1900596 (2020).
[49] J.-S. Zhang and A.-X. Chen, Opt. Express **28**, 36620 (2020).
[50] S. Huang and G. S. Agarwal, Phys. Rev. A **80**, 033807 (2009).
[51] T. Kumar, A. B. Bhattacherjee, and ManMohan, Phys. Rev. A **81**, 013835 (2010).
[52] X.-Y. Lü, Y. Wu, J. R. Johansson, H. Jing, J. Zhang, and F. Nori, Phys. Rev. Lett. **114**, 093602 (2015).
[53] D.-Y. Wang, C.-H. Bai, X. Han, S. Liu, S. Zhang, and H.-F. Wang, Opt. Lett. **45**, 2604 (2020).
[54] R. Schnabel, Phys. Rep. **684**, 1 (2017).
[55] C. K. Law, Phys. Rev. A **51**, 2537 (1995).
[56] M. Aspelmeyer, T. J. Kippenberg, and F. Marquardt, Rev. Mod. Phys. **86**, 1391 (2014).
[57] P. D. Drummond and D. F. Walls, J. Phys. A **13**, 725 (1980).
[58] J. Ma, G. Guccione, R. Lecamwasam, J. Qin, G. T. Campbell, B. C. Buchler, and P. K. Lam, Optica **8**, 177 (2021).
[59] S. Otabe, K. Komori, K. Harada, K. Suzuki, Y. Michimura, and K. Somiya, Opt. Express **30**, 42579 (2022).
[60] See Supplemental Material at http://link.aps.org/supplemental/10.1103/PhysRevLett.132.143602 for additional information on the theory of the Kerr system, data analysis, observed multistable state, and correspondence between optical parametric amplification and Kerr schemes, which includes Refs. [21,28,33–35,55–59,61–67].
[61] A. G. White, J. Mlynek, and S. Schiller, Europhys. Lett. **35**, 425 (1996).
[62] A. Khalaidovski, A. Thüring, H. Rehbein, N. Lastzka, B. Willke, K. Danzmann, and R. Schnabel, Phys. Rev. A **80**, 053801 (2009).
[63] A. Thüring and R. Schnabel, Phys. Rev. A **84**, 033839 (2011).
[64] D. Kelley, J. Lough, F. Mangaña Sandoval, A. Perreca, and S. W. Ballmer, Phys. Rev. D **92**, 062003 (2015).
[65] P. A. Altin, T. T.-H. Nguyen, B. J. J. Slagmolen, R. L. Ward, D. A. Shaddock, and D. E. McClelland, Sci. Rep. **7**, 14546 (2017).
[66] R. W. P. Drever, J. L. Hall, F. V. Kowalski, J. Hough, G. M. Ford, A. J. Munley, and H. Ward, Appl. Phys. B **31**, 97 (1983).
[67] C. M. Caves and B. L. Schumaker, Phys. Rev. A **31**, 3068 (1985).
[68] C. Bosshard, R. Spreiter, M. Zgonik, and P. Günter, Phys. Rev. Lett. **74**, 2816 (1995).
[69] G. I. Stegeman, Quantum Semiclassical Opt. **9**, 139 (1997).
[70] I. Shoji, T. Kondo, and R. Ito, Opt. Quantum Electron. **34**, 797 (2002).
[71] H. Li, F. Zhou, X. Zhang, and W. Ji, Opt. Commun. **144**, 75 (1997).
[72] S. Otabe, Ph. D. thesis, Tokyo Institute of Technology, 2023.
[73] J. Zhang, H. Sun, H. Guo, C. Blair, V. Bossilkov, M. Page, X. Chen, J. Gao, L. Ju, and C. Zhao, Appl. Phys. Lett. **122**, 261106 (2023).